Model of high current breakdown from cathode field emission in aged wire chambers[*][+]

Adam M. Boyarski

Stanford Linear Accelerator Center, M.S. 95, 2575 Sand Hill Rd, Menlo Park, CA 94025, USA

Abstract--**Observing single electron pulses provides insight into the mechanism that leads to sudden high current jumps (breakdown) in aged wire chambers. This single electron activity is found to be consistent with the Fowler-Nordheim equation for field emission of electrons from a cathode surface in a high electric field. The high electric field arises from the positive ion buildup on a very thin insulating layer on the cathode surface. A model is presented to explain the transient behavior of single electron pulses in response to abrupt changes in chamber ionization, as well as the steady state rate during a long term aging run. The model is based on properties of the insulating layer (dielectric constant, conductivity, and hole-mobility) as well as the Fowler-Nordheim equation.**

PACS: 29.40.Cs; 51.50.+v

Keywords: Cathode Aging; Cathode field emission; Chamber aging; Blob model; Self sustaining field emission; SSFE.

I. INTRODUCTION

It is commonly known that drift chambers operating in a high ionization environment while running with certain gas mixtures containing for example hydrocarbons will soon begin to draw current or suffer high current jumps [1] or breakdown that trip the chamber power supply. It is generally believed that breakdown is due to charge build up on a thin insulating dielectric layer on the field wires (cathodes) that reaches a sufficient magnitude to cause a breakdown in the dielectric layer and a release of electrons that provide the current jump. In a previous study [2] it was shown that small pulses (i.e. avalanches from single electrons) were observed to increase in rate before a breakdown occurs in an aged drift chamber test cell. This paper extends those measurements and uses the single electron rate as a probe to understand the mechanism for high current breakdown from aged cathodes. A model for the high current mechanism is presented here.

The model is based on the Fowler-Nordheim equation [3][4] for field emission of electrons from a conducting metal surface in a high electric field, and the work of Malter [5] who showed that a thin insulating film on a cathode that collects positive ions on the surface can produce a high electric field in the film and electron emission from the cathode. Malter made no reference to the earlier work of Fowler-Nordheim that would have undoubtedly explained the high electron currents he observed. This work does make that analogy.

Fowler-Nordheim (FN) derived a formula for the electron field emission current from a metal surface in the presence of a high electric field E (V/m). Fermi electrons in the metal, with work function W (eV), tunnel through the triangular shaped potential barrier illustrated in Fig. 1. A modified FN equation having a slightly rounded

tip in the triangular potential function is calculated in reference [4], and is used here.
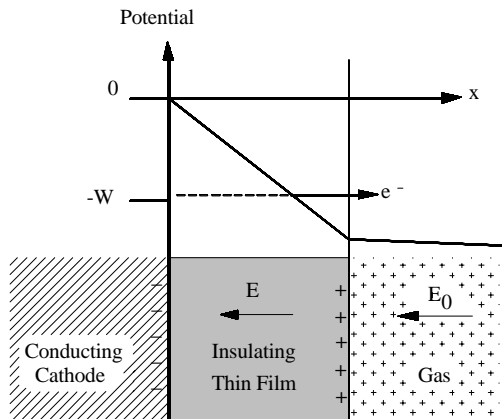

Fig. 1. Thin film Field Emission at a cathode (field wire) surface. Positive gas ions collecting at the insulating film produce a large *E*-field on the conducting cathode surface. Fermi electrons tunnel through the triangular potential barrier into the film, through to the gas.

The field emission current J_{FE} depends on W, E, and other physical constants (m, e, h, etc.). For gold-coated cathode wires, W is 4.3 eV. Since the wire surface is not completely smooth, a factor β (>1) is included for the enhancements in the field at surface protrusions. The modified FN equation for this application is shown in equation 1, where numerical values have been inserted for the physical constants.

$$J_{FE} = 5.4 \times 10^{-5} (\beta E)^2 e^{\frac{-5.43 \times 10^{10}}{\beta E}} \quad (A/m^2) \,..(1)$$

Fig. 2 shows the field emission current J_{FE}, or J-current, as a function of electric field. There is an increase of 24-orders of magnitude in the current as the field changes from 10^9 to 10^{10} V/m, with the largest rate of increase at the lower end. For fields above 5×10^{10}, the dependence approaches a quadratic form.
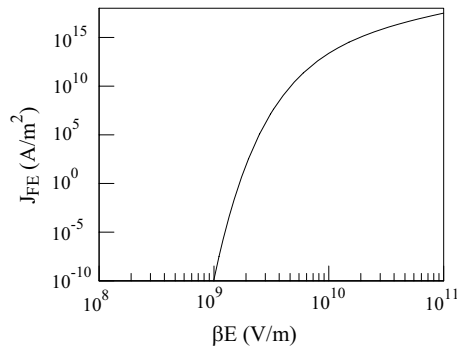

Fig. 2. Fowler-Nordheim field emission current.

The field emission current produces electrons that can penetrate through the insulating film and enter the drift cell, giving single electron avalanches. For example, the test chamber in this study has a cathode area of approximately 10^{-4} m^2 and an avalanche gain of 10^5. At a field of 10^9 V/m where $J_{FE}=1.4 \times 10^{-10}$ A/m^2, the observed current from single electron avalanches would be 1.4×10^{-9} A if the full cathode area participated in field emission. At a field of 1.2×10^9 V/m, the single electron current increases to 1.7×10^{-5} A which is much larger than the maximum possible ionization current in this test chamber.

Some of the field emitted electrons could recombine with positive ion charges collected on the film surface or positive holes that migrate into the film, while transmitted electrons drift to the sense wire and avalanche there. The latter signals provide a probe for studying the underlying mechanism at an aged cathode surface, which is the focus of this study.

II. APPARATUS

The test chamber cell used in this work is shown in Fig. 3. It has one sense, 6 field, and 6 bias wires having diameters 20, 120, and 120 microns and voltages 2050, 0, and 1300 volts respectively, giving fields of 2.4×10^7 V/m on the sense wire (anode) and 1.9×10^6 V/m on the gold coated aluminum field wires. Wires are spaced 1.0 cm apart with a 30.5 cm length. A gas mixture of 80%-Helium 20%-Isobutane was used with no additives so that aging effects could be seen. A Pico ammeter measured the chamber current from the currents in all field wires summed together.
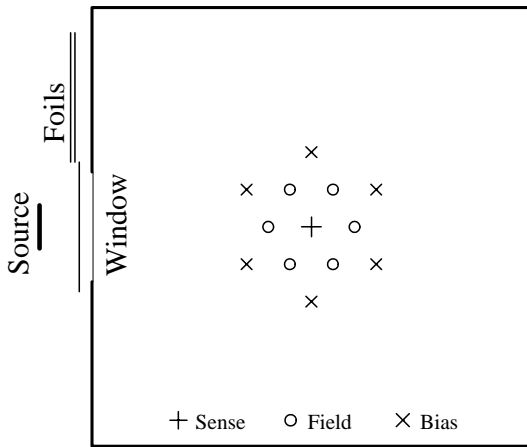
Fig. 3. Test Chamber Drift Cell.

The 5.9 keV gamma rays from a ^{55}Fe source pass through a thin circular window at the mid-length of the chamber, illuminating all the wires over approximately 22 cm of wire length. The maximum ionization occurs at the mid-length of the wire. For a sense wire current I (A), the maximum current per cm of wire is calculated to be 0.077xI (A/cm), giving an effective length of sense wire at the maximum current density to be 13 cm. Foils can be inserted to reduce the ionization level. An 8192-channel analyzer recorded the pulse height spectrum in successive 2-second (or larger) time intervals to measure the history of single electron activity.

The ^{55}Fe pulse spectrum is shown in Fig. 4 together with the shaded regions for the channels used in counting single electrons and the 5.9 keV gamma conversions.
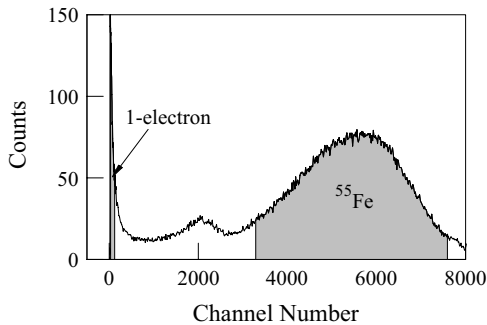

Fig. 4. Pulse height spectrum with shaded regions shown for counting single electrons and ^{55}Fe gamma conversions.

The small peak at approximately channel 2000 comes from 2.1 keV auger electrons from gold produced by gamma absorption in the gold coating on the field wires. During the course of this study two of the gold coated field wires were briefly replaced with uncoated wires. The total gold surface area was thus reduced by 1/3, and it was observed that the height of the 2.1 keV peak was also reduced by 1/3, in agreement with the auger hypothesis.

Since this study is based on measuring single electrons, it is necessary to understand the peak seen in Fig. 4 at small pulse heights. An expanded view of the small pulse region in the spectrum and the shaded region used in counting single electrons is shown in Fig. 5. The peak at low channel numbers is due to gamma conversions at the cell boundaries where only one or a few electrons are collected in the cell and the majority of the conversion electrons are collected by a neighboring cell. Fits to a "Blob" model that calculates the small pulse spectrum from such boundary conversions is also shown in the figure.
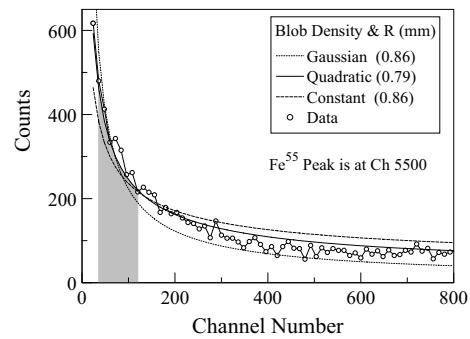

Fig. 5. ^{55}Fe low pulse height spectrum and fits to a "Blob" model showing that conversions at the cell boundary region produce this spectrum (see text).

The "Blob" model assumes that a gamma conversion produces a group of N electrons all contained within a spherical blob of radius R. N is approximately 170 for a 5.9 keV gamma conversion. For conversions near a cell boundary, the blob is sliced in two by the boundary plane and the fractional portion of the blob contained within the cell determines the number of electrons collected by the cell. By moving the conversion point systematically from the outside of a cell through a boundary to the inside of a cell, the probability can be calculated for 1-, 2- … N-conversion electrons being collected in a cell. Essentially, the blob sphere is sliced into N equal-volume pieces, and the width

of the first, second, etc. slice gives the incremental probability for the first, second, etc. electron to be collected. The width is largest for the first slice and so the count for one electron is largest, decreasing monotonically for two, three, etc. The electron distribution or density within the blob must also be taken into account. Fits using three different density models (constant, quadratic, and Gaussian) were made. The quadratic model, which has maximum density at the center decreasing quadratically to zero at radius R, gives the best fit with a blob diameter of 1.6 mm.

Another measurement of single electrons was made by letting room light enter the chamber to produce photo-electrons from the field wires. The spectrum from photo electrons is shown in Fig. 6 together with the chamber noise when no light was present (dark fill), both taken over a 100 second exposure time. The single electron channels (shaded) accept approximately half of the single electrons if it is assumed that the spectrum starts turning downward to zero in the non-recordable region below channel 20.
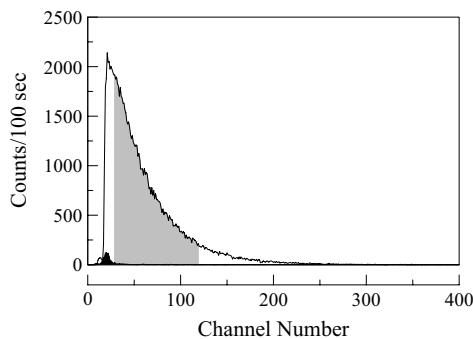

Fig. 6. Single-electron spectrum from photo electrons is shown with the shaded channels used for counting single electrons. The dark-shaded spectrum is the noise seen with the light removed.

The peak in the small pulse spectrum is thus understood, and chamber noise is negligible. Using the cuts in Fig. 4, a spectrum taken at a low source level gives a base line ratio N_1/N_{Fe} for single electrons to ^{55}Fe peak counts to be 0.022. At higher rates, this ratio increases slightly to 0.033 due to pulse pile up or base line shifts. Any increase in this ratio is attributable to field emitted electrons from the cathode.

III. MEASUREMENTS

The previous work [2] presented transient single electron rates as a function of time when a source was suddenly opened at various ionization levels in a damaged chamber. New measurements are presented here of the single electron rates during an aging run starting with a new clean chamber that was aged until increased chamber currents were observed. Both the old data and the new data are used in the modeling section.

A newly rewired test chamber was aged with a 50 mCi ^{55}Fe source until the onset of breakdown. Fig. 7(a) shows the chamber current and Fig. 7(b) the ratio of single electrons per ^{55}Fe conversion taken every 10 minutes for the duration of the aging run.
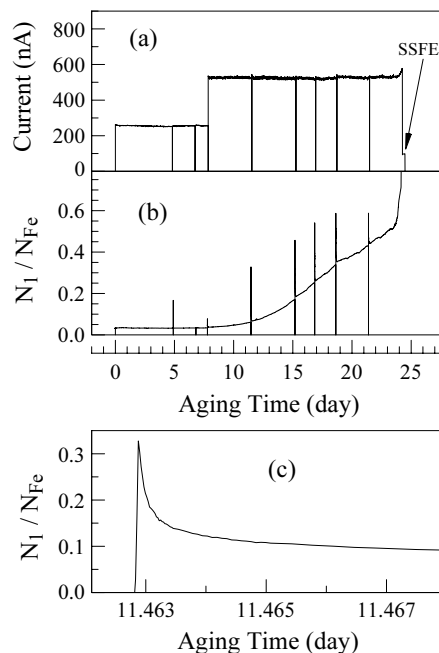

Fig. 7. Aging history of a new drift cell until onset of a self-sustaining current. Plot (a) shows the chamber current. There is a step in day 7 from an increase in HV. The onset of a high current jump is seen in day 24 before the source was turned off. With the source off a self sustaining field emission (SSFE) current remains. Plot (b) is the singles rate per ^{55}Fe. These electrons begin to appear much earlier by day 10 and increase steadily in rate until the sudden jump in day 24. Plot (c) is an expanded view of a singles rate spike during a pause and restart of the aging run in day 11.

The high voltage was elevated in day 7 to speed up the aging process. A gradual increase in the singles ratio is seen after day 10 at an

integrated dose of 0.02 C/cm on the anode wire, reaching 0.55 at day 23, with no visible increase in chamber current. However in day 24, after an integrated dose of 0.07 C/cm, the chamber current as well as the single electron ratio started increasing rapidly. When the source was turned off a self-sustaining current remained.

The aging run was stopped periodically to measure the singles rate at a standard, lower ionization level. The source was closed for 8-10 minutes between runs to allow the chamber to settle to a quiescent state. At each restart of the aging run, there was an initial spike in the singles rate, as shown in Fig. 7(c). Data points were taken more frequently at a restart, every 2 seconds initially and then gradually longer to 10 minutes per point when a steady state was reached. The height of the spike was found to depend on the length of time the source was closed (settling time) prior to starting the run. The chamber voltage during the settling time also affected the spike height. Settling times needed to produce a maximum spike height at turn-on are shown in Table 1 together with the status of the HV and source during the settling time.

Table 1. Settling time needed to produce a maximum spike height at chamber turn-on.

High Voltage	Source	Settling Time (h)
ON	OFF	0.5
OFF	ON	2
OFF	OFF	70

With the HV on and source off, the normal electric field moves the stored charges through the film to the metal surface in a relatively short time (0.5 h). With the HV off and the source on, there is no external field but only a lesser field in the film from the stored charge itself, which moves the stored charges slowly outward to the film surfaces where they are neutralized by the metal on the inner side and by gas ions (electrons) on the outer side of the film. With no HV or source, only ionization from cosmic rays is available for neutralizing the outer side charges, resulting in a long settling time (70 h).

IV. MODELING

It is assumed that an insulating layer or thin film grows on the cathode surface during normal chamber operation from the positively charged gas ions (C_4H_{10}), or fragments (CH_2, etc.) that are attracted there by the electric field, neutralized, and then remain attached to the cathode surface or to the material already present. These ions can combine into long chains creating a polymer layer on the cathode. The thickness of this layer grows with the integrated chamber current as $d = \alpha \int I_{55} dt / 13$, where α is a proportionality constant, I_{55} is the anode current from ^{55}Fe ionization divided by 13 for current per cm of wire.

When an already aged chamber is operating, the instantaneous charge density on the insulating layer is a balance between the incoming ion current at the layer and depletion (discharging currents) within the layer. Depletion may come from ohmic current, or by mobility of holes through the layer, or by recombination of field emitted electrons with holes. On the other hand, field emitted electrons that approach the anode and avalanche there will feed back ions and increase the incoming current. At high enough ionization currents, this positive feedback can sufficiently increase the chamber current into a self sustaining field emission (SSFE) mode, commonly referred to as breakdown or "Malter" mode.

The basic problem for modeling then is finding the correct discharging mechanisms and the amount of feedback.

A charge density Q that is either on the surface or within the layer produces a negative image charge in the metal surface and an electric field $E = Q/\varepsilon$ at the metal surface, where ε is the dielectric constant of the layer material (the relative dielectric constant is defined here as $k = \varepsilon/\varepsilon_0$). The electrostatic field from wire voltages in the cell is E_0 ($\approx 2 \times 10^6$ V/m) at a film-free cathode surface. With a film however, the electrostatic field at the metal surface is E_0/k.

The symbols used in modeling are defined in Table 2. MKS units are used, except for the integrated charge on the sense wire which is in C/cm.

Table 2. Definition of symbols and units used in this document.

Symbol	Description	Units
I_{55}	Anode current from ^{55}Fe ionization.	A
I	Ion current density on field wires.	A/m^2
A_{FW}	Total area of cathode surface collecting ion charge, $I=I_{55}/A_{FW}$.	m^2
E_0	Electrostatic (cell) field at cathode	V/m
E	Total electric field at cathode wire surface	V/m
d	Thickness of insulating film.	m
α	Film thickness per charge (in C/cm) on the anode wire, $d=\alpha \int I_{55} dt /13$.	m-cm/C
k	Relative dielectric constant, ($\varepsilon=k\varepsilon_0$).	
ρ	Volume resistance for holes.	Ω-m
ρ_J	Volume resistance for J current in film.	Ω-m
J_p	Fraction of J current penetrating film promptly.	
μ	Mobility of holes (velocity $v=\mu E$).	m^2/sV
β	Enhancement factor of field at surface protrusion.	
η	Area on cathode of FN field emission	m^2
σ	Recombination cross-section for J current and holes.	m^2
G	Avalanche gain (1×10^5)	
f	Feedback smearing factor, (0-1).	

The chamber gain is 10^5 at low ionization levels, and is assumed to degrade exponentially with higher current levels. Because of avalanche spatial broadening, positive feedback ions do not necessarily return to the exact same spot on the cathode as the original field emitted electron. So if field emission occurs over a very small area (due to a local enhanced field at a surface bump), only a portion of the feedback current contributes to the incoming current at the local point. A smearing factor f is used to reduce the amount of feedback current. The remaining feedback ions are assumed to land in lower E-field regions that are below the field emission threshold, and are ignored in the model.

Applying a step function in ionization provides time dependent single electron rates for studying transient effects, while the long term aging run provides essentially steady-state data at each aging point, if the spike regions in Fig. 7(b) are ignored. An ohmic model that describes the transient behavior is shown next, followed by a steady-state model.

A. Ohmic Discharge (Transient) Model

For a film thickness much less that the radius of the wire, a small area on the wire surface can be considered as a flat parallel plate capacitor with a uniform charge being deposited on the film surface from the incident current density I. A resulting charge Q (C/m^2) on the surface produces an equal and opposite image charge at the metal surface resulting in a uniform field E within the film equal to Q/ε (V/m). The volume resistance ρ of the film material provides a discharge current density E/ρ. The change in surface charge in time dt is then

$$dQ = Idt - \frac{E}{\rho}dt .$$

Expressed in terms of E,

$$dE = (I\rho - E)\frac{dt}{\rho\varepsilon} .$$

Integrating, and using the boundary condition $E=E_0/k$ at $t=0$ gives the solution for E as a function of time,

$$E(t) = \frac{E_0}{k} + I\rho\left(1 - e^{-t/\rho\varepsilon}\right), \quad t > 0 \;\dots(2)$$

The field starts at E_0/k and asymptotically reaches the value $E_0/k+I\rho$ at large times. The $\rho\varepsilon$ term is the time constant of the dielectric layer, equal to the more familiar RC time constant of the layer with capacitance C and resistance R since $\rho\varepsilon=\rho\times d/Area\times\varepsilon\times Area/d=R\times C$.

Since equation 2 is independent of the thickness of the polymer layer, this model cannot fit for d. But it can still be useful for fitting transient data taken over brief intervals of time where the thickness remains the same.

Inserting $E(t)$ into Equation 1 provides the field emission current from the cathode metal surface as a function of time. Two additional parameters η, the area on the metal surface contributing to the field emission and σ, the cross section for recombination of electrons with the positive ion charges on the layer are needed to calculate the observed single electron rate at the sense wire.

A fit of this model to the data taken previously is shown in Fig. 8. The transient N_1/N_{Fe} ratios and the modeled curves are shown for anode currents ranging from 2.1 nA to 13.6 nA. The model does fairly well in describing the onset of the rise in single electron rates. The discrepancy at 2.9 nA is likely due to an improper amount of settling time before making this one measurement. The parameter values from the fit are k=1.3, ρ=4x10^{12} Ω-m, β=136, η=4x10^{-25} m^2, and σ=1.5x10^{-36} m^2 with f set to 1. The very large β factor and small (unphysically small) η area preferred by the fit indicate that the field emission comes from a very small point on the cathode in this highly aged chamber.
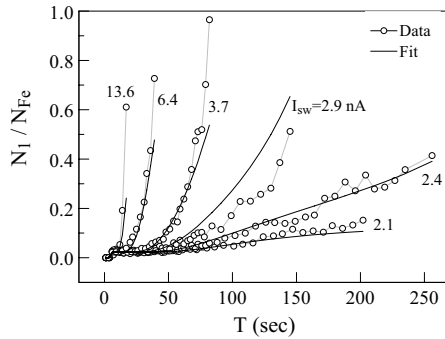

Fig. 8. Single electron rates after opening a source, at various ionization levels (sense wire currents). A fit to a resistive model is shown that uses ε and ρ parameters for the insulating layer, electron-ion recombination, and the Fowler-Nordheim equation.

B. Resistivity + Mobility (Steady State) Model

A model that uses both mobility transfer of positive holes through the insulating layer and an ohmic discharge of the positive charge (holes) provides a slowly increasing E field as a function of d needed to describe the field emission in Fig. 7(b). An analytical equation for this model can be derived in a coordinate system where the cathode metal surface is at $x=0$ and the film thickness extends to $x=d$. A current density I hits the film from the right at $x=d$, and the current density i at location x within the film flows in a negative direction with velocity v that is negative. Two differential equations describe this model, one for E and one for i. The differential equation for the increase in E at the metal surface due to i flowing over time dt is

$$dE = \frac{idt}{\varepsilon} = -\frac{idx}{\varepsilon v} = -\frac{idx}{\varepsilon \mu E} .$$

The decrease in i over time dt from the ohmic discharge current is

$$di = -\frac{dE}{\rho} = \frac{idx}{\rho \varepsilon \mu E} .$$

Differentiating the first equation with respect to x and then eliminating i by use of the second equation leads to the following,

$$E\frac{d^2E}{dx^2} + \left(\frac{dE}{dx}\right)^2 - \frac{1}{\rho\varepsilon\mu}\left(\frac{dE}{dx}\right) = 0 .$$

This differential equation can be solved by letting $p=dE/dx$ and integrating the resulting equation in terms of E and p, and then integrating again the resulting equation in terms of E and x. The boundary conditions at $t=0$ are $x=d$, $E=E_0/k$, and $dE/dx=-I/\varepsilon\mu E_0$.

The solution is given by Equation 3, a transcendental equation for E as a function of x-d, where x is the leading edge of the charge front transported within the film from the transient current step I at $t=0$. Setting $x=0$ provides the steady-state solution when the (surviving) incoming current is transported completely through the film. When x is greater than zero, this model is identical to the model in section A, since no charge is transported through the layer and the accumulated charge in/on the layer is the same as the surface charge in model A.

$$E - \frac{E_0}{k} + \left(\frac{E_0}{k} + I\rho\right)\ln\left(1 - \frac{E - E_0/k}{I\rho}\right) = \frac{x-d}{\rho\varepsilon\mu} \quad ..(3)$$

The steady state solution does not allow determination of the absolute value of d, but only the ratio of d/μ. Additional data, such as a direct measurement of thickness by other means or mobility measurements of the actual film material is required. However, once parameters have been determined for a chamber at one operating condition, the model can still be useful for predicting the wellness of a chamber at different ionization levels or different amounts of accumulated charge.

Equation 3 was checked by a program that stepped in small intervals of time, transporting charge buckets within the film until each charge bucket reaches the metal cathode and neutralizes. At each step, all the charge buckets within the film were depleted by ohmic current. New E fields within the layer as well as on the wire surface were then calculated for the next step in time. The calculated E versus x-d from the stepping program agreed well with the analytic calculation of E from equation 3 when small stepping times ($\leq$0.1 s) were used.

Fig. 9 shows the steady-state field as a function of d, using the same parameters found

in the fit that follows. Inserting E into the FN equation results in a field emission current that increases almost linearly with d above 30 nm. Feedback must also be added in the field calculation.
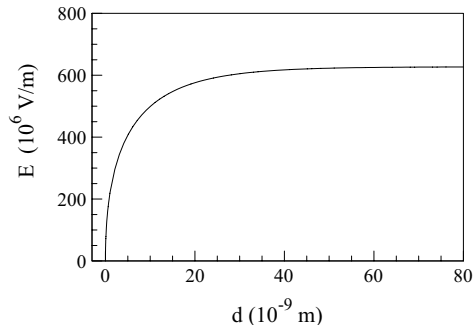

Fig. 9. The electric field from a charged thin film on the cathode as a function of film thickness, when the charge is depleted both by resistivity and mobility.

A computer program was written to compute R_1, the modeled values of N_1/N_{Fe}, at each data point in Fig. 7(b). At each data point, d is calculated from the integrated anode current (C/cm) times a proportionality constant α. The α parameter was chosen to give a thickness between the extremes of <2 um (would be seen optically if larger than this) and at least 10-100 atomic layers (d>1-10 nm) to acquire bulk properties. The incoming current I is initially set to the ionization current, and the program then computes in sequence the values for E, J_{FE}, J_1 (the field emission current density at the cathode that reaches the anode), and the feedback current. An augmented I current with the feedback included is calculated for the next iteration. The iterations stop when I reaches a stable value. The modeled ratio R_1 is then calculated from the ratio of total avalanche-amplified field emission current ($G\eta J_1$) to the ionization current, and the baseline as

$$R_1 = 0.033 + \frac{G\eta J_1}{I_{55}}$$

The parametric model fit is shown in Fig. 10. Some parameters were set to preconceived values while others were allowed to vary. The relative dielectric constant was set to 2.3, the value for polyethylene that might mimic the polymer layer with its CH_2 chains. A factor of 2 was chosen for β for a rather smooth gold wire surface, with no whiskers in a new chamber that had not yet operated in SSFE mode.
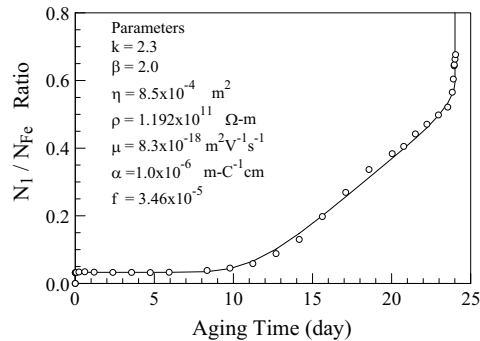

Fig. 10. A fit of the measured single electron rates during an aging run to a model that depletes the charge build up on a thin film on the cathode by both resistive and mobility discharging described in the text.

The fit for this model had difficulty converging because of the enormous increase in field emission with only slight changes in some parameter values. Good starting values had to be found manually before attempting a fit. It is quite possible that there are other equally good solutions.

This model reproduces the data very well. It follows the observed flat, no field emission region before day 9, and the subsequent onset of field emission at an accumulated charge of 0.02 C/cm. The model follows the almost linear increase through to the onset of SSFE at 0.07 C/cm in day 24. The model then jumps rapidly in day 24 in agreement with the data.

This test chamber ran ~3.5 times longer than the time for first evidence of single electrons, so single electron monitoring provides a means of predicting a chamber's breakdown long before it occurs. This monitoring must be done while the chamber is operating smoothly and constantly at a high ionization level, otherwise transient single electron spikes would hamper the steady state determination.

C. Transient Spike

Neither of the above models can explain the spike seen in Fig. 7(c). The spike feature appears to require a sudden burst of charge followed by a slow discharge. Adding a resistance parameter ρ_J in the passage of field-emitted electrons through the film provides such a mechanism. As the E field increases with time beyond the field emission threshold, there is a sudden surge of electrons. The resistance limits the discharge rate of these electrons, trapping the electrons momentarily in the film and decreasing the E field on the wire surface, thereby reducing

subsequent field emission. As these electrons discharge slowly, equilibrium is reached between the incoming ionization current and the field emitted electrons. A second new parameter J_p was also added for the fraction of field emitted electrons that promptly escape through the film unhindered through cracks or tunnels in the polymer layer. A fit with this model to an observed spike is shown in Fig. 11. All the parameters shown in Fig. 10 were used without modification except for η, which had to be increased. This model fits the data well in the spike region, although it does not follow the drop in rate at larger times.
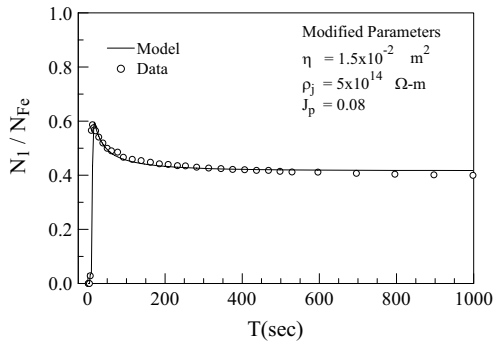

Fig. 11. A transient single electron spike in Fig 7(b) at day 19 with a fit to a model in which the discharge rate of the field emitted electron current is limited by resistance in the film. Parameters are the same as in the previous figure except for η and two new ones shown.

A simultaneous fit of the spike region and the steady state region with a single set of parameters was not found. Both the ρ_J and η parameters have to be larger in the transient region than the steady state region. The reason for this is not known.

V. AGING WITH WATER

Although a water additive has been shown to prevent high chamber currents [1][2], it would be useful to know if polymer growth still occurs when running a chamber with a water additive.

A second almost new test chamber was used to measure this, by aging it with a gas mixture of helium:isobutane (80:20) and 0.35% water for 28 days. The chamber was then allowed to dry for two months with a water-free (80:20) gas flow until the single electron transient spike no longer changed in runs taken several days apart. The amount of aging could then be seen in two

different ways, 1) by comparing the single electron activity before and after the aging run in this chamber, and 2) by comparing the single electron activity in this aged chamber with that in the chamber aged without water.

For the first method, a chamber current of only 6 nA after aging was seen to give the same transient spike height as a chamber current of 70 nA before the aging run, showing clearly that the chamber had aged while running with the water additive. The results from the second method can be seen in Fig. 12, where the single electron transient rates are shown for both chambers operating at the same 55 nA current. The water-aged chamber with an integrated dose of 0.080 C/cm on the anode shows approximately the same level of single electron activity as the non-water-aged chamber at a dose of ≈0.045 C/cm, indicating that the build up rate with water was approximately 55% that of the aging rate with no water.
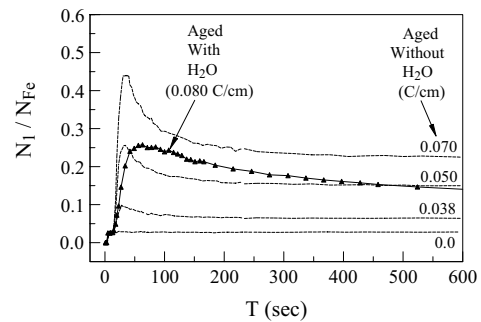

Fig. 12. Transient single electron activity after aging a chamber with a water additive to an integrated anode charge of 0.080 C/cm, compared to activity in a chamber aged without water.

The rise and fall times of the spike for the "Aged with H_2O" case are longer than the "Aged without H_2O" case. The reason for this is unknown, but considering these are two different chambers it could be due to different film properties in the region of field emission in one chamber compared to that in the other chamber. Somewhat longer rise and fall times were also observed initially in the second chamber before the aging run, so it can not be concluded that water was responsible for changing the film properties.

VI. CONCLUSIONS

This article provides new insights for the high current breakdown in drift chambers operating at high ionization levels. Chamber breakdown arises from the enormous amount of electron field emission when the electric field in an insulating thin film at the cathode reaches a certain threshold. These electrons then avalanche and increase the ionization already present in the chamber, leading to high current jumps and self-sustaining field emission (SSFE).

Chambers operating constantly and steadily at a high ionization level with no additive in the gas could be monitored for the first sign of problems by measuring the single electron rate at each wire, looking for increases in this rate with operating time. When single electrons were first detected in the test chamber, the chamber continued to run smoothly for 3.5 times longer before the SSFE condition was reached. In this test chamber, the SSFE condition was reached when the (corrected) single electron counting rate became comparable to that from ^{55}Fe gamma conversions.

Cathode aging can be summarized as follows:
- Positive ions in the gas collect on the cathode, neutralize, and stick to the cathode, building an insulating layer. This build up occurs during normal chamber operation. A water additive does not prevent this build up, although it may reduce the rate by $\approx 50\%$.
- Newly arriving positive charge is discharged both resistively in the film as well as by mobility of positive holes through the film. This transitory charge in the film creates a high E field on the metal cathode surface.
- The magnitude of the E field depends on the layer thickness as well as the film's properties (ρ, ε, μ).
- The high E field produces Fowler-Nordheim electron field emission from the cathode. Once a certain E threshold is reached, further small increases in the field produce a very rapid increase in emitted electrons.
- These electrons feed back to the anode where they avalanche and add to the positive ion current, leading to SSFE in the chamber.

Transient behavior of single electrons to a sudden increase in chamber ionization in an aged chamber can be described by resistive discharges only, while the steady-state single electron rate requires that charge be removed both by hole-mobility as well as ohmic discharging.

This article is based on measurements in a helium-isobutane gas, but the conclusions should be applicable to any gas that can produce an insulating coating on cathode wires.

Chambers that already show signs of field emission in a high ionization environment should turn on the high voltage slowly to allow the transient single electron current to decay (order of minutes) rather than reach the SSFE threshold.

Acknowledgments

References

[1] J. Va'Vra, Review of Wire Chamber Aging, Nucl. Instr. And Meth. A252, 547-563 (1986).

[2] A. M. Boyarski, Additives That Prevent Or Reverse Cathode Aging in Drift Chambers With Helium-Isobutane Gas, Nucl. Inst. And Meth. A515, 190-195 (2003).

[3] R. H. Fowler and L. Nordheim, Electron Emission in Intense Fields, Roy. Soc. Proc. London, 119A, 173-181 (1928).

[4] R. H. Good and E. W. Muller, Field Emission, in "Handbook der Physik", Springer Verlag, Berlin, 21, 176-231 (1956).

[5] L. Malter, Thin Film Field Emission, Phys. Rev. 50, 48-58 (1936).